Approximations for the Stellar atmosphere

(We are assuming radiative equilibrium – transfer of energy by radiation only)

In the atmosphere, $r \approx R_*$, so $L(r) = 4\pi r^2 F(r)$,

but $L(r)$ is fixed, no nuclear energy generation.

Then F = constant $= L / 4\pi R_*^2$. $\boxed{\frac{dF}{d\tau} = 0}$ radiative eq. $F = \int F_\nu d\nu$

(We are also ignoring any time dependences).

(We are also ignoring any time dependence and assuming no light incoming at the surface (i.e. not close binary etc) is constant)

(Note: F = constant does not imply $F_\nu(r)$ is constant)

We adopt a linear form for $S(\tau)$, $S_0 + S_1 \tau$. (Eddington–Barbier approx)

We assume a semi-infinite atmosphere, so

$$I(0,\mu,\nu) = \int_0^\infty (S_0 + S_1\tau)\, e^{-t/\mu}\, dt/\mu$$

$(\mu > 0)$

then $$I(0,\mu,\nu) = -S_0 e^{-t/\mu}\Big]_0^\infty + S_1\mu \int_0^\infty x e^{-x} dx$$

$$\boxed{I(0,\mu,\nu) = S_0 + S_1\mu = S(\tau=\mu)} \quad \boxed{\mu > 0}$$

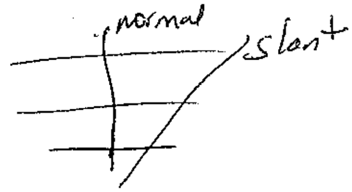

For normal incidence, $\mu = 1$

I is given by S at $\tau = 1$ along the line of sight (at $\tau = \mu$ for a slant path)

The surface flux is then

$$\pi F_\nu(0) = \int_0^{90} I(0,\mu)\, \mu\, d\Omega = \int_0^1 (S_0 + S_1\mu)\mu\, d\mu (2\pi)$$

$$\pi F_\nu(0) = \left(S_0 + \frac{2}{3} S_1\right) \pi$$

$$\boxed{F_\nu(0) = S_0 + \frac{2}{3} S_1 = S_\nu(\tau = 2/3) = B_\nu(\tau = 2/3)}$$

The effective optical depth for the formation of the continuum flux is $\tau = 2/3$.

Summary of Eddington - Barbier relationships

$$S_\nu = B_\nu = S_0 + S_1 \tau \quad \text{(assumed)}$$

$$I_\nu(0,\mu) = S_\nu(\tau = \mu) \leftarrow \text{limb darkening law}$$

$$F_\nu(0) = B_\nu(\tau = 2/3)$$

This gives no information on $T(r)$ or $T(\tau)$.

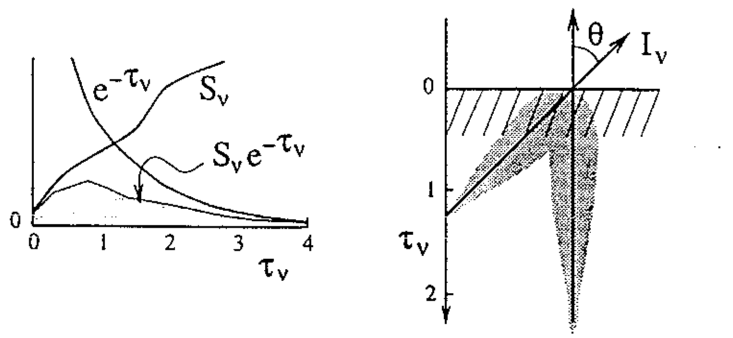

Figure 1.3: The Eddington-Barbier approximation. Left: the integrand $S_\nu \exp(-\tau_\nu)$ measures the contribution to the radially emergent intensity $I_\nu(\tau_\nu\!=\!0, \mu\!=\!1)$ from layers with different optical depth τ_ν. The value of S_ν at $\tau_\nu = 1$ is a good estimator of the area under the integrand curve, *i.e.*, the total contribution. Right: for a slanted beam the characteristic Eddington-Barbier depth is shallower than for a radial beam; it has $\tau_\nu = \mu$.

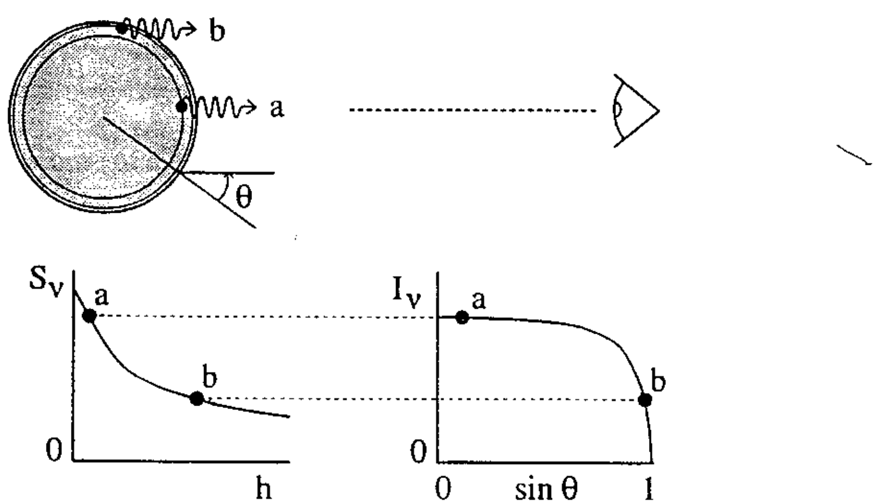

Figure 1.4: Solar limb darkening. The viewing angle θ increases with the fractional radius $r/R_\odot = \sin\theta$ of the apparent solar disk. The emergent intensity samples shallower layers towards the limb, with smaller source function. The final drop at $r/R_\odot = 1$ marks the viewing angle at which the sun becomes optically thin. Note that substantial decrease of $\mu = \cos\theta$ is reached only close to the limb, for $r/R_\odot = \sin\theta = \sqrt{1-\mu^2}$ close to unity.

The Grey Atmosphere

very complicated. Too hard. Assume k_ν is constant

$$dI_\nu = j_\nu \rho \, ds - k_\nu \rho I \, ds \qquad \text{(plane // atmosphere)}$$

$$\cos\theta \frac{dI_\nu}{d\tau_\nu} = I_\nu - \frac{j_\nu}{k_\nu} = I_\nu - S_\nu \qquad (1)$$

For the grey case, $\tau_\nu = \tau$, $k_\nu = k$ (constant opacity ind of ν)

$$\frac{d}{d\tau}\iint I_\nu \cos\theta \, d\Omega \, d\nu = \iint (I_\nu - S_\nu) \, d\Omega \, d\nu$$

$$\frac{d}{d\tau} F = 4\pi J - 4\pi S = 0$$

Since flux is constant with depth.

Hence $\boxed{J = S}$ $\qquad J = \int J_\nu \, d\nu$

This only works because $\frac{dF}{d\tau} = \frac{d}{d\tau}\left(\int F_\nu \, d\nu\right)$, not $\frac{dF_\nu}{d\tau_\nu}$!

In LTE, $S_\nu = B_\nu$, so $S = B = \int B_\nu \, d\nu = \sigma T^4$

Now multiply (1) by $\cos\theta$ & then integrate

$$\frac{d}{d\tau}\int I \cos^2\theta \, d\Omega = \int I \cos\theta \, d\Omega - \underbrace{\int S \cos\theta \, d\Omega}$$

this term is 0, S is independent of angle

$$\frac{d\, 4\pi K}{d\tau} = 4\pi H \quad \text{(flux)}$$

$$\boxed{K = H\tau + \text{constant}}$$

$$\mu \frac{dI}{dz} = I - S = I - J = \cancel{\int I}$$

$$= I - \int_{-1}^{1} I \frac{d\mu}{2}$$

$$\boxed{\mu \frac{dI}{dz} = I - \int_{-1}^{1} I \frac{d\mu}{2}}$$

Still can't solve this to get $T(z)$

Deming & (Grey pg2)

Very simple model (Bowers ~~&~~, §5.7)

(5)

Constant L, $r = R_*$ plane ∥ layers, κ = mean grey /unit length op.

$F\kappa/c$ = absorbed momentum of photons/sec, and $\frac{dP_{rad}}{dz}$ = force of rad. pressure

$$F = \frac{c}{\kappa}\frac{dP_{rad}}{dz} = c\frac{dP_{rad}}{d\tau}$$

$$F = \sigma T_{eff}^4 \qquad c\frac{dP_{rad}}{d\tau} = \sigma T_{eff}^4 \text{ (constant)}$$

depends on local temp.

$$P_{rad} = \frac{4}{3}\frac{\sigma}{c}T^4 = \frac{\sigma}{c}T_{eff}^4(\tau + q)$$

constant of integration

Need to find q, must approximate.

Assume at R_*, All rad. flows outward,

$B_\nu = T_{eff}$, at $\boxed{\frac{1}{2}}$ of BB flux at R_* (surface of star)

$$P_{rad}(0) = \frac{2}{3}\frac{\sigma T_{eff}^4}{c} \qquad \text{So } q = \frac{2}{3}$$

$$\frac{4}{3}T^4 = T_{eff}^4\left[\tau + \frac{2}{3}\right]$$

$$\boxed{T^4 = \frac{3}{4}T_{eff}^4\left[\tau + 2/3\right]} \quad \boxed{\text{(~~Approximate~~) Solution!!}}$$

$$T^4(\text{Surface}) = \frac{1}{2}T_{eff}^4, \qquad \boxed{T(0) = 0.84\,T_{eff}}$$

$$\boxed{T(\tau = 2/3) = T_{eff}}$$

$\tau = 2/3$ is effective depth

T(τ=0) Sun ~4850 K

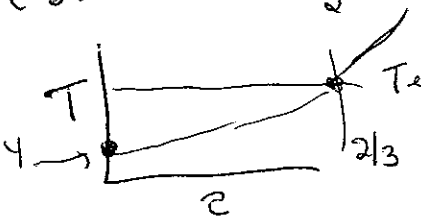

Need actual κ to integrate $\frac{dP}{d\tau} = \frac{g}{\kappa}$

$$\frac{dP}{dr} = -\rho g \rightarrow$$

So $$\boxed{T^4_{(\tau)} = T_{eff}^4 \left(\frac{1}{2} + \frac{3}{4} \tau \right)}$$

Grey case, approximate solution.

$$T(\tau = 0) = T_{eff} \left(\frac{1}{2} \right)^{1/4} = 0.84\ T_{eff}$$

Spectral lines therefore cannot be infinitely deep

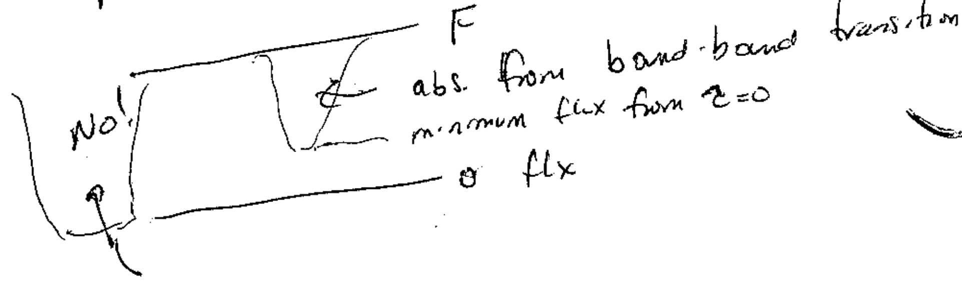

Grey Atmosphere

Grey case can be solved analytically, $q(\tau)$ determined, but its very messy math.

Use the grey solution to begin iterating in the non-gray case, with a suitable choice of mean opacity.

Limb Darkening In the Sun

The solar disk is darker at its edges because

$\frac{dT}{dr} < 0$ (T increases inward)

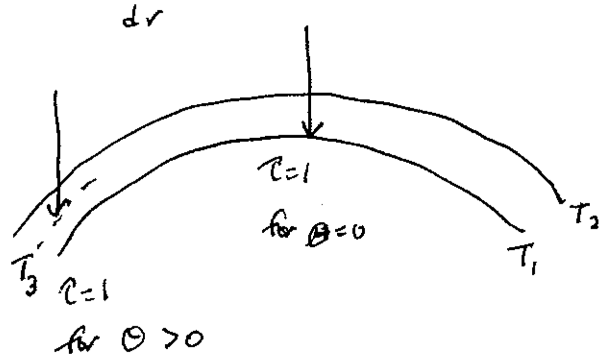

$T_1 > T_3 > T_2$

Slant optical depths in a slab:

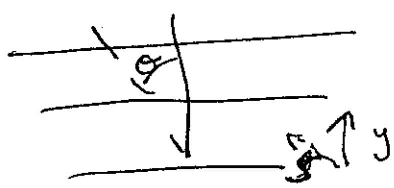

$ds = dy/\cos\theta$

s is along the ray

At center of disk see σT_1^4, near the edge see σT_3^4, which is smaller ($T_3 < T_1$)

At uv wavelengths, $\tau = 1$ is in the corona so $\frac{dT}{dr} > 0$, and we see limb brightening!

$\eta_\nu \rho \, ds = \eta_\nu \rho \, dx/\cos\theta$ emission at depth x

$$dI_\nu = \eta_\nu \rho \frac{dx}{\cos\theta} e^{-\tau/\cos\theta}$$

$$d\tau = \kappa \rho \, dx \qquad dI_\nu = -\frac{\eta_\nu}{\kappa_\nu} \frac{d\tau}{\cos\theta} e^{-\tau/\cos\theta}$$

Consider a grey atmosphere, so $S_\nu = J_\nu$

$$dI_\nu = -J(\tau)\,\frac{d\tau}{\cos\theta}\,e^{-\tau/\cos\theta}$$

$$I(0,\theta) = -\int_\infty^0 J(\tau)\,e^{-\tau/\cos\theta}\,\frac{d\tau}{\cos\theta}$$

$$= \int_0^\infty H\,(2+3\tau)\;e^{-\tau/\cos\theta}\,d\tau/\cos\theta$$

approx. grey solution

$$= 2H\underbrace{\int_0^\infty e^{-\tau/\cos\theta}\,d\tau/\cos\theta}_{1} + 3H\int_0^\infty \tau\,e^{-\tau/\cos\theta}\,d\tau/\cos\theta$$

$$= 2H + 3H\cos\theta$$

$$\boxed{I(0,\theta) = H\,[2+3\cos\theta]}$$

You can also get this from the formal solution

$$I(0,\mu) = \int_0^\infty S(t)\, e^{-t/\mu}\, \frac{dt}{\mu}$$

$$= \int_0^\infty \frac{3}{4} F\left(\tau + \frac{2}{3}\right) e^{-t/\mu}\, \frac{dt}{\mu}$$

$$= \frac{3}{4} F\left(\mu + \frac{2}{3}\right) \qquad (\mu = \cos\theta)$$

This is the same as the above solution.

$$\frac{I(0,\mu)}{I(0,1)} = \frac{\frac{3}{4}F(\mu + 2/3)}{\frac{3}{4}F(5/3)} = \frac{3}{5}(\mu + 2/3)$$

↑ normal, $\theta = 0°$; $\cos\theta = 1$

$$= 0.4 + 0.6\,\mu = 0.4 + 0.6\cos\theta$$

θ	$\mu = \cos\theta$	$I(0,\mu)/I(0,1)$
0	1	1
15	0.97	0.98
30	0.87	0.92
45	0.71	0.82
60	0.50	0.70
75	0.26	0.56
90	0.0	0.40

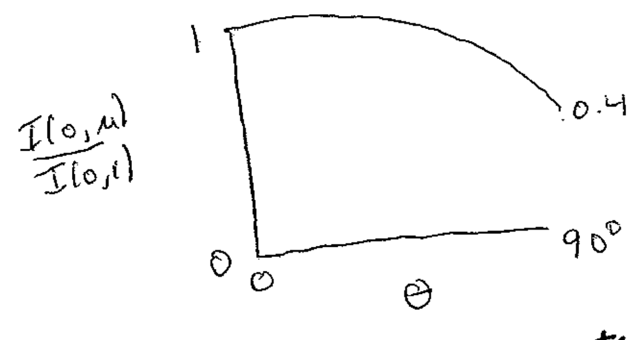

Good agreement suggests radiative equilibrium prevails in the upper layers of the solar atmosphere.

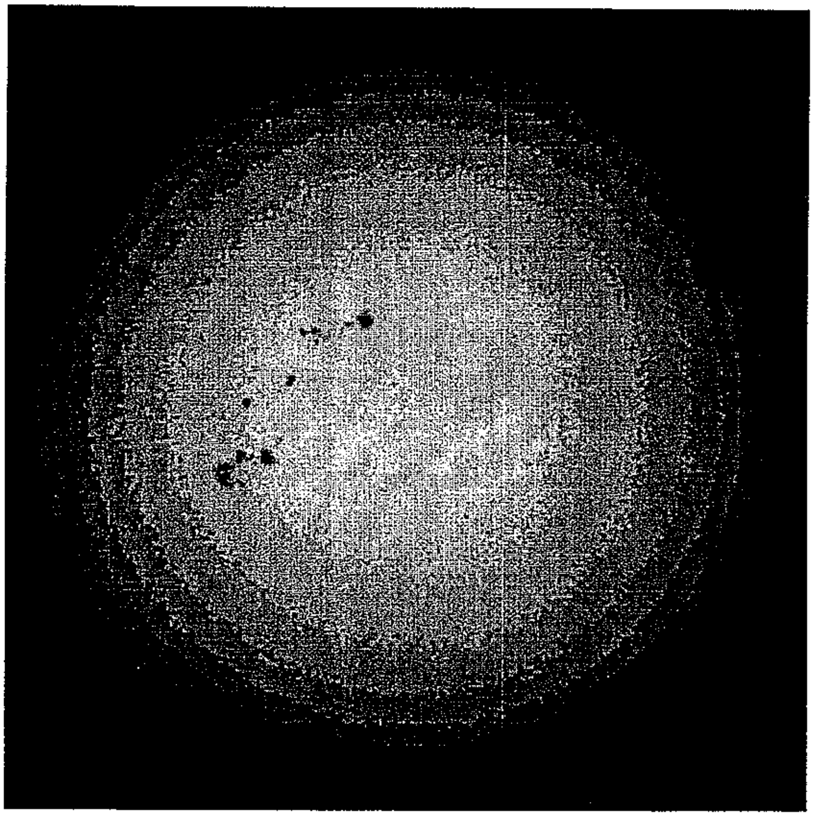

http://www.bbso.njit.edu

Big Bear Solar Observatory

Latest images – full disk observations

Oct 14, 1999

Schematic for
Limb Darkening

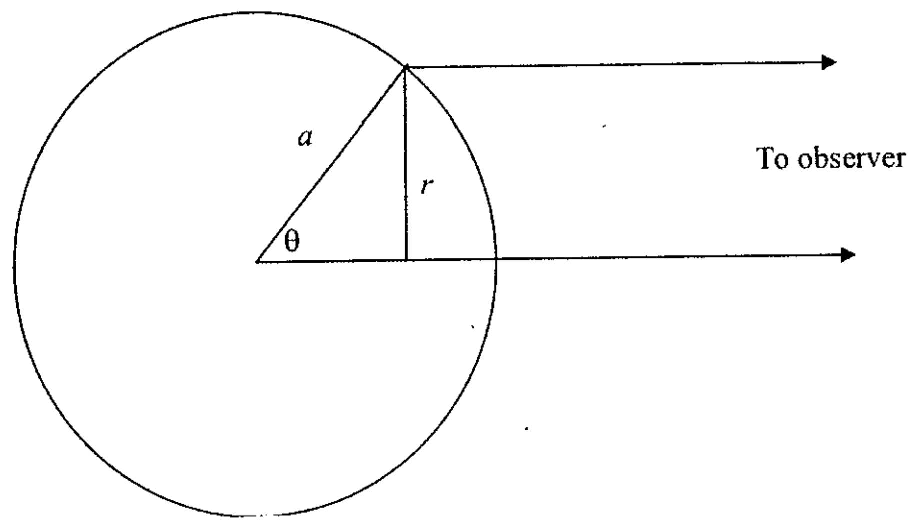

Astron. Astrophys. 333, 338–342 (1998)

ASTRONOMY
AND
ASTROPHYSICS

Wavelength dependency of the Solar limb darkening

A + A 333, 338, 1998

D. Hestroffer[1] **and C. Magnan**[2,3]

[1] Astrophysics Division, Space Science Department of ESA, ESTEC, Postbus 299, 2200 AG Noordwijk, The Netherlands
[2] GRAAL, Université de Montpellier II, F-34095 Montpellier Cedex 5, France
[3] Collège de France, Paris

Received 19 September 1997/ Accepted 27 October 1997

Abstract. A single parameter model of the mean Solar limb-darkening is presented. This empirical law has the advantage to represent the limb darkening over a large spectrum at least as well as a quadratic or logarithmic law. Since it is less sensitive than high degree polynomial laws, it is recommended for subsequent analysis of average limb-darkening variations and comparisons.

Consider another empirical law for the model of the normalised brightness distribution across the disc:

$$I(\mu) = 1 - u(1 - \mu^{\alpha}) \quad ; \quad (u, \alpha) \in \mathbb{R}^2 \tag{1}$$

This simple law has the property of yielding the shape of the normalised intensity with only a few parameters. The fit to the observational data given by Petro et al. (1984, their Table 2B) is shown in Fig. 2. The approximation is better than $\pm 1\%$, and hence is competitive with for instance the logarithmic law:

2 *Model Curves*

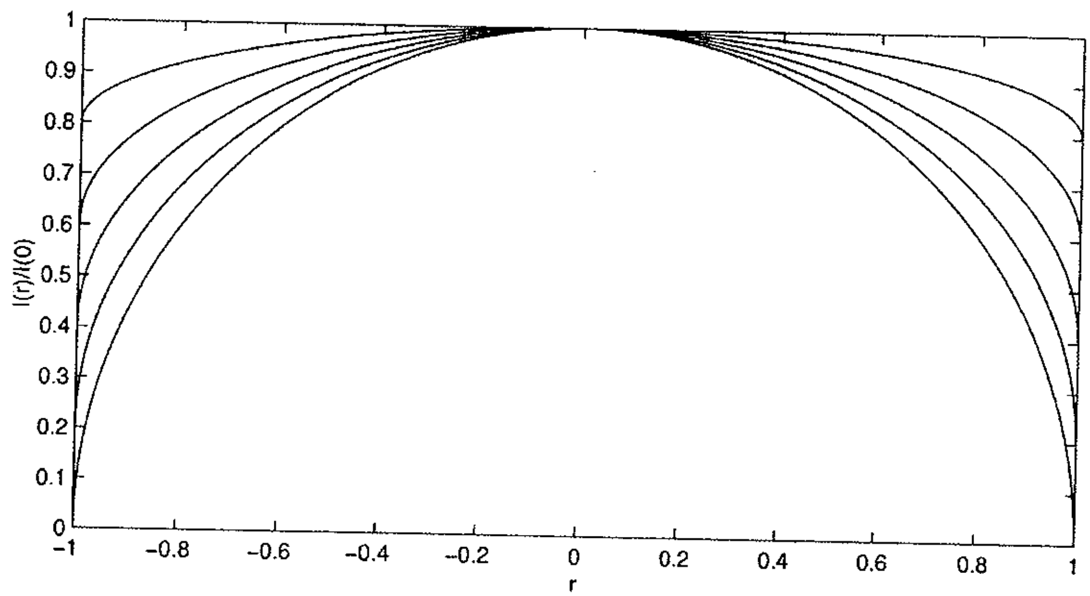

FIGURE VI.2

Equation 6.1.1 for six limb darkening coefficients, from the lowest curve upwards, u = 1.0, 0.8, 0.6, 0.4, 0.2 and 0.0. The "curve" for the last of these (no limb darkening) is formed from three of the boundary lines. The curve for $u = 1$ is a circle. The radius of the disc is taken to be 1, $r = 0$ is the centre of the disc and $r = \pm 1$ is the limb.

Table 1. Coefficients of the polynomial fits in Fig. 1

$\lambda = 5798.8$ nm	a_0	a_1	a_2	a_3	a_4	a_5
PS	0.30505	1.13123	-0.78604	0.40560	0.02297	-0.07880
NL	0.28392	1.36896	-1.75998	2.22154	-1.56074	0.44630
Δa_k	-0.021113	0.23773	-0.97394	1.81594	-1.58371	0.52510

Fits to
Solar observations

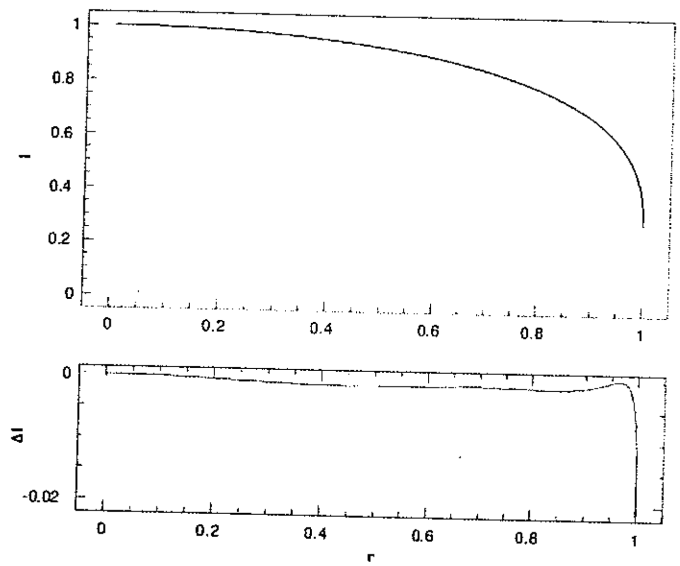

Fig. 1. Normalised intensity following NL and PS, indistinguishable on the graph (top), and residuals NL-PS (bottom). The agreement between the two representations is excellent for $r \leq 0.9$. This is not reflected by the coefficients of the polynomial functions (see Table 1)

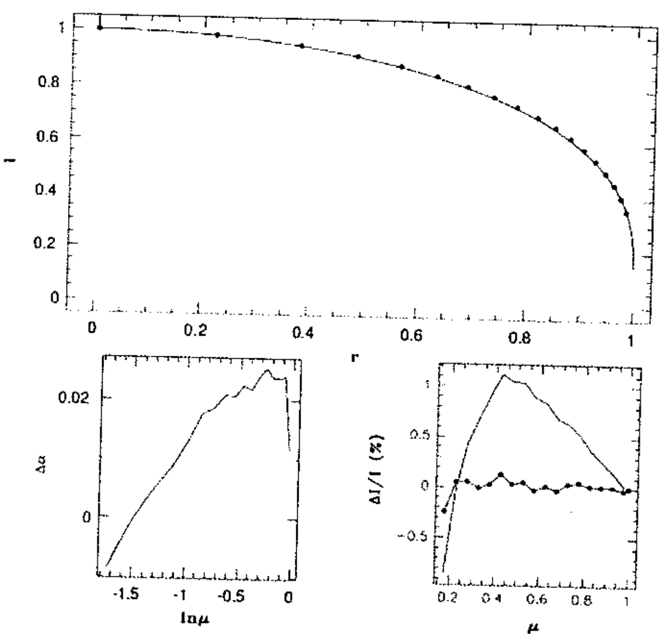

Fig. 2. Average drift scan of the Sun fitted by a power law of Eq. (1) with $u = 0.85$ and $\alpha = 0.8$. Filled circles correspond to observations of Petro et al. (1984). The residuals are given on the lower right panel for the 6 parameters approximation of Petro et al. and the fit of this paper. See text for an explanation of the characteristic quantity $\Delta\alpha$

Table 2. Exponent of the limb-darkening function versus wavelength for PS, PSW and NL data

PS		NL	
λ [nm]	α	λ [nm]	α
303.327	0.967	303.327	0.939
306.982	0.942		
310.843	0.904	310.843	0.914
320.468	0.867	320.468	0.871
329.897	0.816	329.897	0.817
338.953	0.779		
349.949	0.753	349.947	0.763
356.352	0.749		
362.650	0.714		
365.875	0.684	365.875	0.695
374.088	0.751	374.086	0.750
377.992	0.739		
385.202	0.808		
390.928	0.790	390.915	0.791
395.425	0.782		
398.815	0.744		
401.970	0.741	401.970	0.751
406.944	0.731		
411.723	0.693		
416.320	0.712	416.319	0.724
421.905	0.705		
427.930	0.670	427.930	0.682
431.645	0.643		
443.885	0.652	443.885	0.649
445.125	0.648	445.125	0.646
454.355	0.633		
456.792	0.620		
457.345	0.631	457.345	0.628
461.510	0.614		
468.306	0.600		
471.900	0.582		
477.435	0.588	477.427	0.594
481.157	0.580		
483.075	0.569		
490.560	0.575		
492.905	0.569	492.905	0.570
498.090	0.573		
503.800	0.554		
510.210	0.539		
519.930	0.529	519.930	0.538
526.535	0.542		
533.460	0.522		
541.760	0.511	541.760	0.514
552.200	0.503		
559.950	0.502	559.950	0.496
569.560	0.482		
579.880	0.473	579.880	0.477
587.430	0.465		
601.015	0.464		

PS		NL	
λ [nm]	α	λ [nm]	α
610.975	0.452	610.975	0.447
620.590	0.434		
632.600	0.429		
640.970	0.420	640.970	0.428
649.250	0.413		
660.400	0.401		
669.400	0.396	669.400	0.407
679.140	0.397		
691.600	0.388		
700.875	0.383	700.875	0.386
710.425	0.368		
719.925	0.375		
729.675	0.372		

Wavelength
Dependency

PSW		NL	
λ [nm]	α	λ [nm]	α
740.460	0.359		
748.710	0.348	748.710	0.361
770.820	0.342		
789.900	0.324		
811.760	0.325	811.760	0.333
828.410	0.315		
847.510	0.307		
869.600	0.303	869.600	0.311
903.380	0.284		
948.850	0.280	948.850	0.292
997.920	0.270		
1046.700	0.262	1046.600	0.274
1098.950	0.246	1098.950	0.260
1158.350	0.242		
1197.750	0.231		
1251.500	0.220		
1299.000	0.219		
1307.400	0.194		
1338.100	0.208		
1339.400	0.194		
1402.000	0.196		
1430.100	0.163		
1457.900	0.183		
1493.100	0.166		
1500.100	0.172		
1564.200	0.146		
1580.300	0.165		
1595.100	0.143		
1622.200	0.162		
1642.000	0.137		
1659.800	0.154		
1670.000	0.145		
1686.000	0.126		
1695.700	0.138		
1704.300	0.151		
1719.800	0.155		
1748.300	0.146		
1789.100	0.136		
1798.400	0.150		
1813.800	0.134		
1894.500	0.146		
1925.000	0.151		
1969.200	0.125		
2022.000	0.132		
2100.200	0.136		
2185.500	0.133		
2216.300	0.127		
2312.800	0.127		
2401.800	0.123		

How to make a non-grey atmosphere look grey

choose correct Mean opacity (Mihalas pg 57)

non-grey | grey

$$\mu \frac{\partial I_\nu}{\partial z} = \kappa_\nu (S_\nu - I_\nu) \quad (1) \qquad \mu \frac{\partial I}{\partial z} = \bar{\kappa} (J - I)$$

flux

$$\frac{\partial}{\partial z}(H_\nu) = \kappa_\nu (S_\nu - J_\nu) \quad (2) \qquad \frac{\partial H}{\partial z} = 0$$

$$\frac{\partial K_\nu}{\partial z} = -\kappa_\nu H_\nu \quad (3) \qquad \frac{dK}{dz} = -\bar{\kappa} H$$

Flux weighted mean opacity

$$\int_0^\infty \kappa_\nu H_\nu \, d\nu = \bar{\kappa} H \qquad \int H_\nu d\nu$$

This satisfies equation (3), but not necessarily eq. (2)

Also H_ν is not known in advance & hence must iterate then calculate H_ν.

This choice is not commonly used.

Rosseland mean opacity — fine the correct integrated flux

$$\int_0^\infty \frac{1}{\kappa_\nu} \frac{\partial K_\nu}{\partial z} = \int_0^\infty H_\nu d\nu = \text{desired flux} = \frac{1}{\bar{\kappa}} \frac{dK}{dz}$$

Now assume the radiation field is almost isotropic, almost a black body, so

$$\frac{1}{\bar{\kappa}_R} = \frac{\int \frac{1}{\kappa_\nu} \frac{\partial B_\nu}{\partial T} d\nu}{4\sigma T^3} \longleftarrow \int \frac{\partial B_\nu}{\partial T} d\nu = \frac{\partial}{\partial T}(\sigma T^4)$$

Since $\frac{1}{\bar{K}} \propto \frac{1}{K_\nu}$
This is a harmonic mean, with highest weight given to regions with smallest opacity.

Using τ_{Ross} we recover at large depths the correct asymptotic solution of the transfer equation + the correct $T(\tau)$

Radiative Eq in Atmosphere

Mihalas pg 48

33

$$\frac{dF}{d\tau} = 0 \qquad \underbrace{\frac{dF}{dt}}_{\text{time}} = 0$$

total energy removed from beam

$$= \int_0^\infty d\nu \int d\Omega \; k(\vec{r},\nu)\, I(\vec{r},\theta,\phi,\nu)$$

$$(K_\nu \text{ ind. of angle}) = 4\pi \int_0^\infty k(\vec{r},\nu)\, J(\vec{r},\nu)\, d\nu$$

total energy delivered to beam =

$$\int d\nu \int d\Omega \; \eta(\vec{r},\nu) = 4\pi \int_0^\infty k\, S(\vec{r},\nu)\, d\nu$$

$$\frac{\eta}{k} = S$$

$$\boxed{\begin{aligned} &4\pi \int_0^\infty (\eta - kJ)\, d\nu = 0 \quad \text{at all locations } \vec{r} \\ &4\pi \int_0^\infty k(\vec{r},\nu)\left[S(\vec{r},\nu) - J(\vec{r},\nu)\right] d\nu = 0 \end{aligned}}$$

$$\boxed{\text{LTE} \quad I = J = S = B_\nu(T)}$$

true approximately locally

$\Rightarrow T$ PS defines all level populations, ion. eq. etc

from Le Blanc

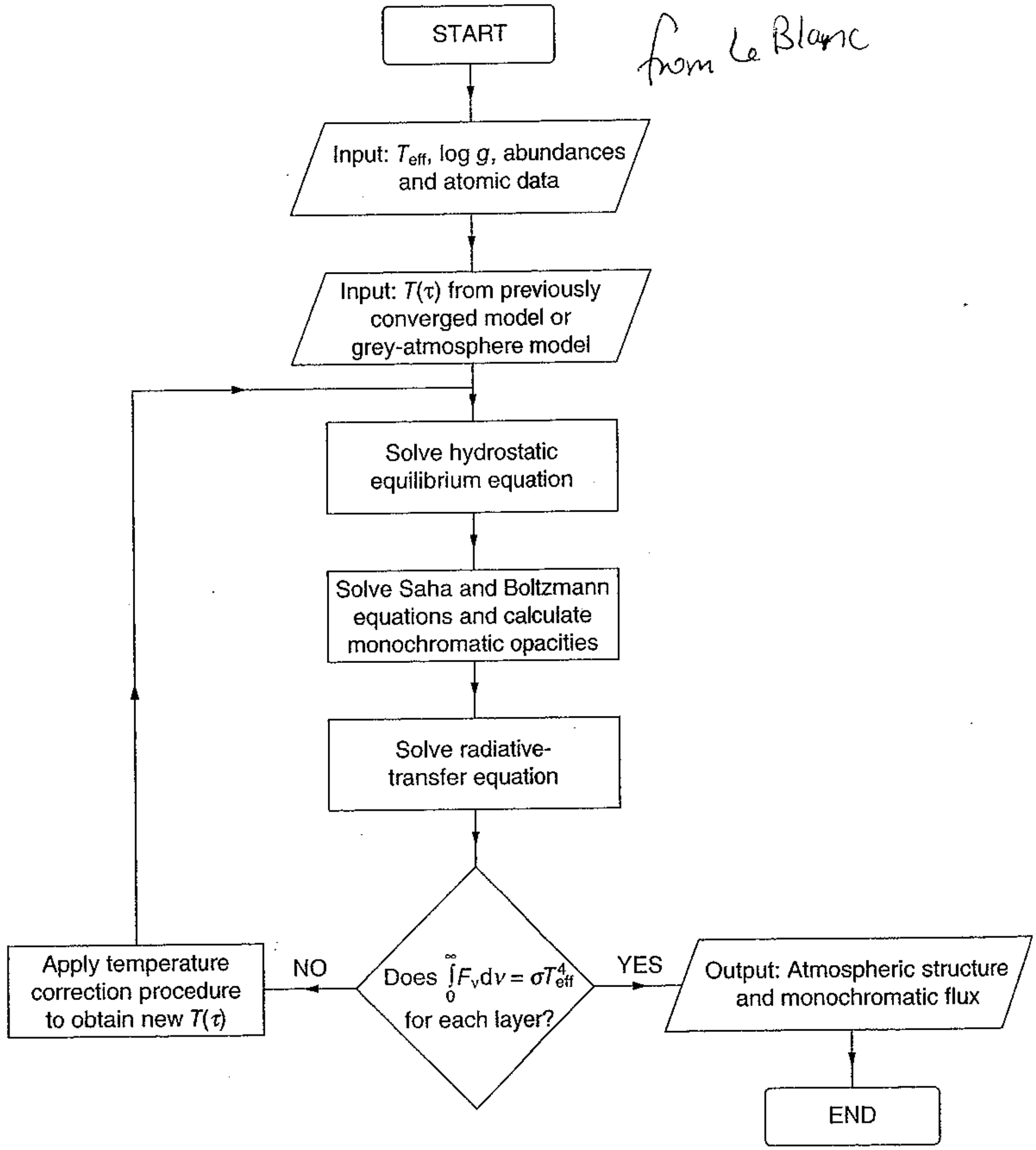

Figure 4.19 Flowchart of the algorithm used for atmospheric modelling of a plane-parallel model. Once the radiative-transfer equation is solved, radiative pressure that is not mentioned in this figure or in the text may also be included in the hydrostatic equilibrium equation for subsequent iterations (see optional Section 3.12). Figure reproduced and adapted with permission from François Wesemaël.

from Le Blanc

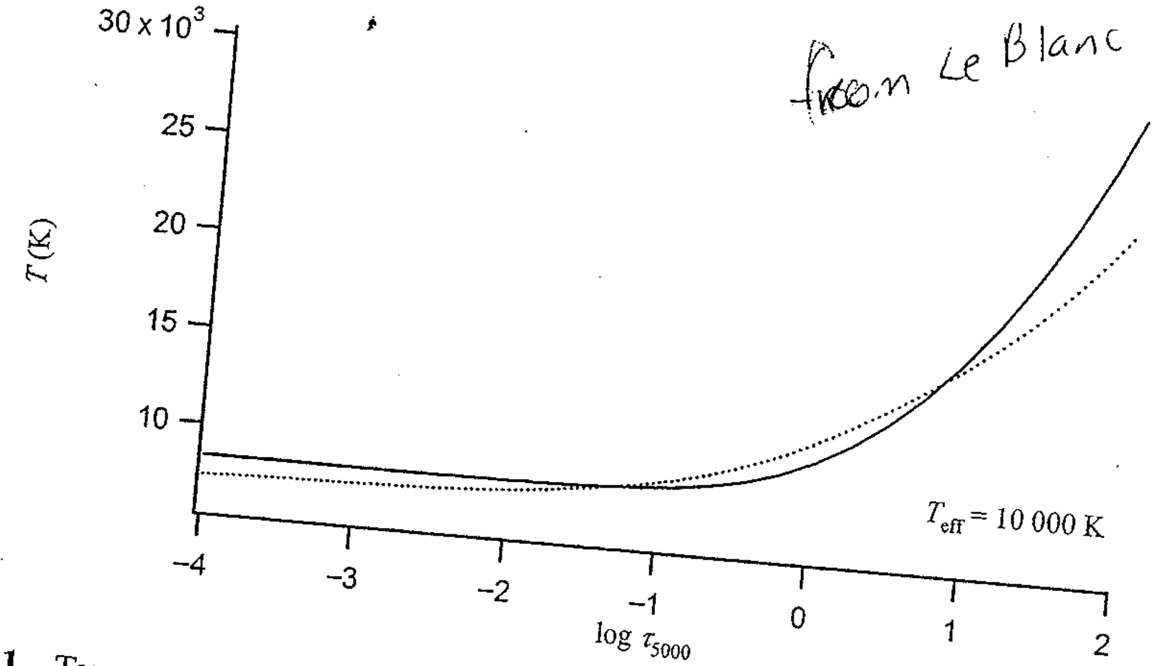

Figure 4.1 Temperature profile of a detailed atmospheric model with T_{eff} = 10000 K, $\log g = 4.0$ and solar abundances (solid line) and the one for a grey atmosphere (dotted line), as a function of the optical depth calculated at 5000 Å.

from Le Blanc

Teff 19000K
log(g) 4.0

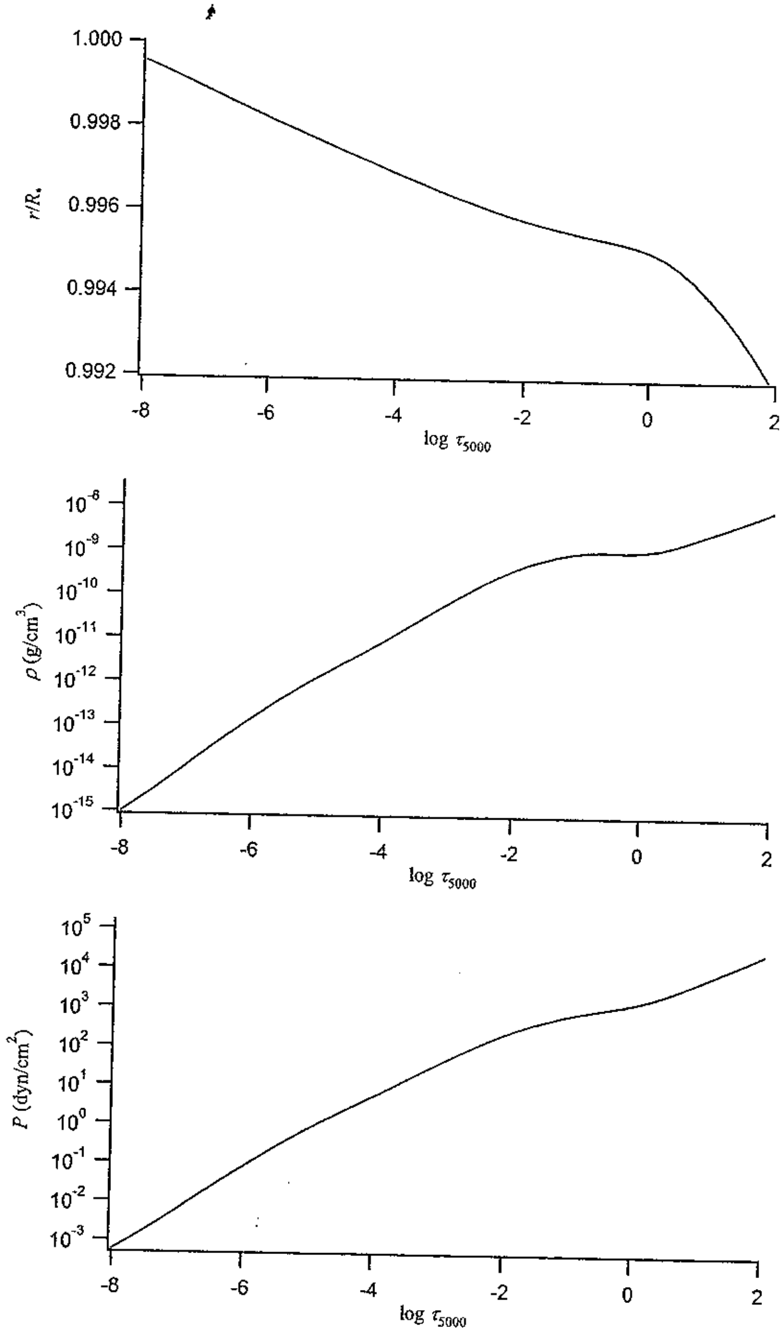

Figure 4.20 The ratio of the local radius to that of the stellar radius, density and pressure as a function of optical depth calculated at 5000 Å for a plane-parallel model atmosphere with $T_{\rm eff} = 10\,000$ K, $\log g = 4.0$ and solar abundances. The temperature profile for this stellar atmosphere model is shown in Figure 4.1.

GRIDS OF MODEL STELLAR ATMOSPHERES

The Grand Master, Robert Kurucz (kurucz.harvard.edu)
ATLAS code, initial implementation mid 1970s, under
  continuous development/ugradeing
  (take a look at papers directory, atlas9atlas12.pdf)
  ATLAS12 is described in Kurucz 2005
  1d plane parrallel layers, LTE

Hauschildt, Allard, Ferguson, Baron & Alexander,
      1999, ApJ, 525, 871 Phoenix/NextGen Models
  Hauschildt's code is called PHOENIX
   updated in 1999 to support spherical geometry
   PHOENIX code at version 16 in 2013
  See Husser, Wende-von Berg, ..., Hauschildt, 2013, arXiv:1303.5632
  published in Astronomy & Astrophysics, 2013

Gustafsson, Bell, Eriksson \& Nordlund, 1975, A&A, 42, 407
 his code is called MARCS
Gustafsson, Edvardsson, Eriksson et al, 2008, A&A, 486, 951
  added spherical symmetry

ATLAS9 and MARCS models for the APOGEE project can be found at
 http://www.iac.es/proyecto/ATLAS-APOGEE

Sz. Meszros, Allende-Prieto, Edvardsson et al, New ATLAS9 and
   MARCS model atmosphere grids for the APOGEE Experiment
   2012 (see arXiv:1208.1916) (ApJ, 2012)

Baraffe, Homeir, Allard & Chabrier, 2015, arXiv:1503.04107
   update of Baraffe. Chabrier, Allard & Hauschildt, 1998, A&A, 337, 403
   Models for very low mass (hence very cool) dwarfs
   (they use modified PHOENIX/NEXTGEN models)

Non-LTE models for hot stars:
Code TLUSTY developed by Hubeny
I. Hubeny & Lanz, 1995, ApJ, 439, 875
Lanz & Hubeny 2003, 2003, ApJS, 146, 417
latest version is described in
Lanz & Hubeny, 2007, ApJS, 169, 83 (see arXiv:0611891)

==

3D MODEL ATMOSPHERES

time dependent hydrodynamic 3D Models with Temporal Averaging
  (i.e. a better treatment of convection than the mixing length theory)

development led by Marti Asplund
see the series of papers on the STAGGER-grid
paper 1 (methods and general properties)
Magic, Collet, Asplund et al, arXiv:1302.2621

paper 2: Temporal Averaging and Spectral Line Formation
arXiv:1307.3273

Also Trampedach, Asplund, Collet et al, 2013, arXiv:1303.1780

These require enormous amounts of computer time to
calculate and large model grids are not available
==

LIBRARIES OF SYNTHESIZED STELLAR SPECTRA

An extensive library of 2500-10,500 A synthetic spectra, 2005,
Munari, Sodro, Castelli & Zwitter, 2005, A&A,
Kurucz codes, resolving power 20,000, 11500, 8500 and 2000,
1 and 10 A/pixel, 3500 < Teff, 47,500 K etc.

A High Resolution Stellar Library for Evolutionary Population Synthesis
L. Martins, Gonzalez Delgado, Leitherer, Cervino & Hauschildt,
2005, MNRAS, 358, 49
1654 stellar spectra, 3000-7000 A, 0.3 A resolution,
Kurucz + Phoenix + non-LTE hot models
www.iaa.csic.es/~rosa or (www.astro.iag.usp.br/~lucimara/library.html-not working)

Evolutionary Stellar Population Synthesis at High Spectral
Resolution: Optical Wavelengths, 2005, MNRAS, 357, 945
Delgado, Cervino, Martins ... Hauschildt
Astro-ph/0501204, SSP models, 0.3 A resolution, 3000 to
7000 A, 2x,1x,0.5x,1/10 Solar metallicity, ages 1 to 17 Myr
using Geneva and Padua tracks.
www.iaa.csic.es/~rosa and www.iaa.csic.ed/~mcs/Sed@

Title: Interpreting Spectral Energy Distributions from Young Stellar Objects.
  I. A grid of 200,000 YSO model SEDs
Authors: Thomas P. Robitaille, Barbara A. Whitney, Remy Indebetouw, Kenneth
  Wood, Pia Denzmore
Comments: 69 pages, 28 figures, Accepted for publication in ApJS. Preprint with
  full resolution figures available at http://www.astro.wisc.edu/protostars/

BLUERED theoretical synthestic spectra, Bertone 2001, 2003
2001, PhD thesis, Milan University, Italy
2003, in Galaxy Evolution: Theory and Observatoins, Rev.Mex. Astrophys.
    Conf Series, 17, 91
galaxy spectra

UVBLUE -
library of theoretical stellar spectral energy distributions
www.bo.astro.it/~eps/uvblue/uvblue.html
850 to 4700 A at spectral resolution of 50,000. Kurucz models.
1800 models used.
Rodriguez-Merino, Chavez, Bertone and Buzzoni, 2005, Astro-ph/0504307
indices from these Chavez, Bertone, Buzzino...,2007,
   ApJ, 657, 1046 astro-ph/0611722

A library of high resolution synthetic stellar spectra from 300nm
to 1.8 microns with solar and alpha-enhanced composition
Coelho, Barbuy, Melendez, Schiavon & Castilho, 2005, A&A,
Astro-ph/0505511

Spectral models for solar-scaled and alpha-enhanced stellar
populations - Coelho, Bruzual, Charlot, Weiss, Barbuy
& Ferguson, MNRAAS, 2008, astro-ph/0708.2790

Prospects for population synthesis in the H band: NeMO grids
of stellar atmospheres compared to observations
(comparison of synthesized spectra for individual stars)
Fremaux, Kupka, Boisson, Joly & Tsymbal, 2005,

Astro-ph/0511125 (A&A)

Recio-Blanco, de Laveryny, Plez, 2005, ESA technique note,
RVS-ARB-001 (for Gaia), see Recio-Blanco, Bijaoui & de Laverny,
MNRAS, 2006

C.Gummersbach and A. Kaufer - Synthetic Spectra of Main Sequence B-stars
from 3000 to 10,000 A, nice plots come up.
www.lsw.uni-heidelberg.de/cgi-bin/websynspec.cgi
(found reference in 2nd page of Huang and Gies, 2006, ApJ, 648, 591)

Palacios, Begran, Josselin, Martins, Plez, Belmas & Lebre
arXiv:1003.4682
POLLUX: a database of synthetic stellar spectra
resolution is 150,000
http://pollux.graal.univ-montp2.fr

Title: New H-band Stellar Spectral Libraries for the SDSS-III/APOGEE survey
Authors: O. Zamora, D. A. Garcia-Hernandez, C. Allende Prieto, R. Carrera, L. Koesterke, B. Edvardsson, F. Castelli, B. Plez, D. Bizyaev, K. Cunha, A. E. Garcia Perez, B. Gustafsson, J. A. Holtzman, J. E. Lawler, S. R. Majewski, A. Manchado, Sz. Meszaros, N. Shane, M. Shetrone, V. V. Smith, G. Zasowski
Comments: 45 pages, 11 figures; submitted to AJ

The Sloan Digital Sky Survey--III (SDSS--III) Apache Point Observatory Galactic Evolution Experiment (APOGEE) has obtained high resolution (R $\sim$ 22,500), high signal-to-noise ($>$ 100) spectra in the H$-$band spectral region ($\sim$1.5$-$1.7 μm) for about 146,000 stars in the Milky Way galaxy. We have computed specific spectral libraries with effective temperature ($T\rm{_{eff}}$) ranging from 3500 to 8000 K for the automated chemical analysis of the survey data. The spectral libraries, used to derive stellar parameters and abundances from the APOGEE spectra in the SDSS--III data release 12 (DR12), are based on ATLAS9 model atmospheres and the ASSϵT spectral synthesis code. We present a second set of stellar spectral libraries based on MARCS model atmospheres and the spectral synthesis code Turbospectrum. The ATLAS9/ASSϵT ($T\rm{_{eff}}$ = 3500$-$8000 K) and MARCS/Turbospectrum ($T\rm{_{eff}}$ = 3500$-$5500 K) grids of synthetic spectra cover a wide range of metallicity ($-$2.5 $\leq$ [M/H] $\leq$ $+$0.5 dex), surface gravity (0 $\leq$ log g $\leq$ 5 dex), microturbulence (0.5 $\leq$ ξ $\leq$ 8 km s^{-1}), carbon ($-$1 $\leq$ [C/M] $\leq$ $+$1 dex), nitrogen ($-$1 $\leq$ [N/M] $\leq$ $+$1 dex), and α-elements ($-$1 $\leq$ [α/M] $\leq$ $+$1 dex) variations, having thus seven dimensions. We compare the ATLAS9/ASSϵT and MARCS/Turbospectrum spectral libraries and we apply both of them to the observed H$-$band spectra of the Sun and the K2 giant Arcturus, as well as to a selected sample of well-known giant stars observed at very high-resolution. The new APOGEE synthetic spectral libraries are publicly available online and can be employed for chemical studies in the H$-$band using other high-resolution spectrographs.
\\ (http://arxiv.org/abs/1502.05237 , 4168kb)

compiled by Judy Cohen, Oct 2015